

PAPER • OPEN ACCESS

Influence of wind-wave characteristics on floating wind turbine loads: A sensitivity analysis across different floating concepts

To cite this article: Likhitha Ramesh Reddy *et al* 2024 *J. Phys.: Conf. Ser.* **2767** 062030

View the [article online](#) for updates and enhancements.

You may also like

- [UK perspective research landscape for offshore renewable energy and its role in delivering Net Zero](#)
Deborah Greaves, Siya Jin, Puiwah Wong et al.
- [Similarity laws of the wind wave and the coupling process of the air and water turbulent boundary layers](#)
Yoshiaki Toba
- [3D printed self-propelled composite floaters](#)
Soheila Shabaniverki, Antonio Alvarez-Valdivia and Jaime J. Juárez



ECS The Electrochemical Society
Advancing solid state & electrochemical science & technology

ECS UNITED

247th ECS Meeting
Montréal, Canada
May 18-22, 2025
Palais des Congrès de Montréal

Showcase your science!

Abstracts due December 6th

Influence of wind-wave characteristics on floating wind turbine loads: A sensitivity analysis across different floating concepts

Likhitha Ramesh Reddy¹, Dimitra Karystinou¹, Daniel Milano²,
John Walker², Axelle Viré¹

¹Faculty of Aerospace Engineering, Delft University of Technology, Delft, Netherlands

²Offshore Renewable Energy Catapult, Glasgow, UK

E-mail: l.rameshreddy@tudelft.nl

January 2024

Abstract. Floating offshore wind turbines experience different operating conditions, such as wind and wave inflow characteristics. Accurate prediction of the loads acting on the floating wind system is essential for the system design and optimisation. However, there are a lot of uncertainties with the modelling input variables for time domain simulation tools such as OpenFAST to represent various hydro-aerodynamic and structural properties. The primary objective of this work is to identify the critical input parameters for different damage-equivalent load outputs for two substructure types: OC3 Hywind Spar and OC4 DeepCwind semisubmersible. The same rotor-nacelle assembly and tower (the NREL 5MW reference turbine) are used in both case studies. A sensitivity analysis based on the damage equivalent loads of six output quantities was conducted with 8 or 10 input parameters (depending on the floater). The dependent parameters were conditionally parameterised based on the independent inputs, such as wind speed and wind-wave misalignment.

The outcomes of this work show that the floater type affects the sensitivity levels of wave characteristics and hydrodynamic drag coefficients with no significant influence on the turbulence intensity, as expected. Further, the drag coefficient for spar-buoy configuration significantly influences mooring line tension compared to the semisubmersible because of their drag-dominant slender structure. The current velocity is the most dominating parameter for the mooring loads, irrespective of the floater type. While wave characteristics also influenced some turbine loads, it was almost independent of the floater type. Furthermore, the choice of the hydrodynamic model does not affect the sensitivity level rankings. A convergence study on the number of starting points was conducted to ensure a global sensitivity approach. As seen in this study, the results are floating platform-specific. This study provides valuable insight into design-driving input parameters, characterising substructure-specific wind-wave influence.

Keywords: elementary effects, damage equivalent loads, OpenFAST, spar, semisubmersible

1. Introduction

The design of floating offshore wind turbine (FOWT) systems requires evaluations against several design load cases (DLCs) as outlined by the International Electrotechnical Commission (IEC) 61400-1 and 61400-3 standards [1], [2]. A margin of safety is considered to account for the uncertainty in determining the ultimate and fatigue loads, as well as the uncertainty in



predicting system properties and variation in the operating conditions of the FOWTs. For design optimisation to reduce the system's levelised cost of energy (LCOE), it is crucial to understand the effect of wind and wave characteristics as well as system parameters.

Sensitivity analysis approaches have been applied in offshore wind, focusing predominantly on the wind resource assessment [3] and the LCOE-based design optimisation of the floating support structure design [4, 5]. A few studies have been conducted that are focused on substructure structural damping [6] and aerodynamic damping [7] but are applied only to monopile configurations. Limited attention is devoted to sensitivity analysis of environmental conditions and modelling characteristics. Ziegler et al. [8] conducted Monte Carlo simulations to study the influence of wave fatigue loads under different wave characteristics for a 4MW turbine atop a monopile foundation. For onshore wind, a study by Robertson et al. [9] performed sensitivity analysis on wind inflow characteristics for an NREL 5MW baseline turbine. Wiley et al. [10] extended that work to an NREL 5MW baseline wind turbine mounted on the OC4-DeepCwind semisubmersible. To our knowledge, this is the only work that addresses the effect of both wind and wave parameters. The current study expands on that work by Wiley et al. [10] and studies the impact of different substructure types. The objective of the research is two-fold: firstly, to examine the effect of wind-wave characteristics on the semisubmersible and spar floating substructure types, both supporting an NREL 5MW reference turbine and secondly, to understand the influence of the physical model fidelity.

The remainder of this paper is organised as follows. Section 2 describes the sensitivity analysis approach, input variables selected with the parameter bounds, and the output variables analysed. Further, the results are presented in Section 3 with the conclusions being drawn in Section 4.

2. Methodology

2.1. Floating offshore wind turbine system

This paper presents a comparative study between two distinct floater configurations: spar-buoy and semisubmersible. For this study, the NREL 5MW reference turbine [11] is selected with the OC3-Hywind spar-buoy [12] and OC4-DeepCwind semisubmersible support-structure [13], as depicted in Figure 1. Both the FOWTs use catenary mooring systems for station keeping. By keeping the rotor aerodynamics constant, the analysis hones on identifying the implications of substructure design on the sensitivity analysis.

The availability of a pre-existing sensitivity study on the NREL 5MW turbine atop the semisubmersible drives the choice of turbine. This necessitates the comparison with a different floater configuration (spar-buoy).

2.2. Numerical model

Time domain simulations are performed using an aero-servo-hydro-elastic tool, OpenFAST, to obtain the dynamic response of the floating wind turbine system. TurbSim is used to generate the stochastic turbulent inflow wind. Within TurbSim, the IEC Kaimal spectral model, as detailed in IEC 61400-1 [1], and the power-law wind profile are specified. OpenFAST uses different modules to analyse different dynamics of the system, as listed below:

- **AeroDyn** evaluates aerodynamic forces on the turbine using the Blade Element Momentum (BEM) method with unsteady aerodynamics.
- **HydroDyn** calculates hydrodynamic forces on the floating platform using the potential flow theory in combination with Morison drag elements to capture viscous effects. The irregular wave field is generated using the JONSWAP spectrum. A depth-independent model is employed for defining currents.

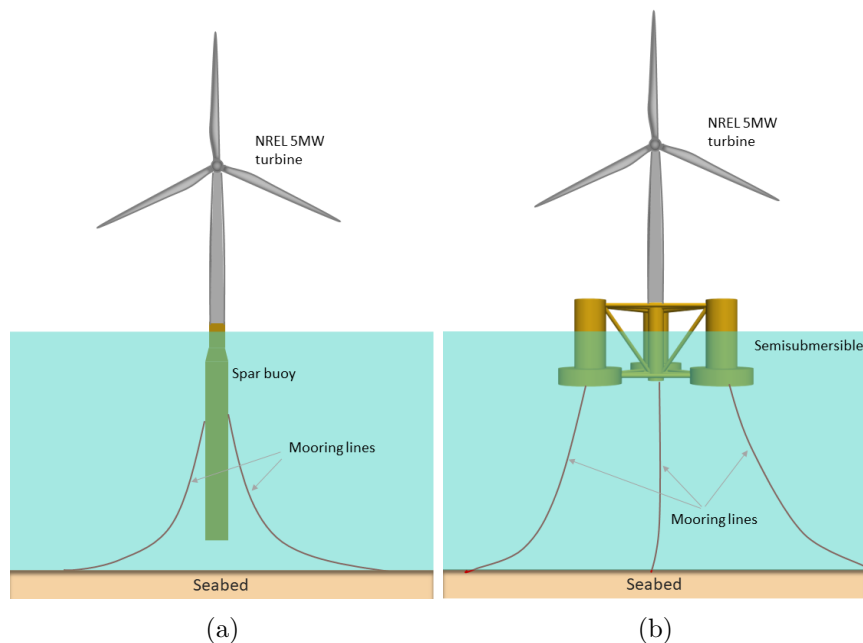


Figure 1: Floating offshore wind turbine configurations selected for the sensitivity analysis: NREL 5MW reference turbine with a) OC3-Hywind spar platform and b) OC4-DeepCwind Semisubmersible platform

- **MoorDyn** models the mooring system with a lumped-mass approach, where the dynamics are discretised over the length of the mooring lines.
- **ElastoDyn** computes the structural dynamics, treating substructures as rigid while the tower and blades are flexible.
- **ServoDyn** implements the controller for the NREL 5MW turbine using a bladed-style dynamic link library, adopting variable-speed generator torque and collective blade pitch control.

The IEC 61400-1 standard [1] recommends a 60-minute long simulation or six 10-minute stochastic realisations. 10-minute long simulations are run with 2 minutes of transient removed from the output time series. Wiley et al. [10] showed that a transient period of 1 min is sufficient for such simulations. Ten repetitions of such 10-minute stochastic realisations are performed.

2.3. Sensitivity analysis methodology

Sensitivity analysis can be performed through various approaches depending on factors like computational time, the number of input variables assessed, and their variability range. In this case, a screening method called the elementary effects (EE) method is used. The overview of the sensitivity analysis methodology is represented in Figure 2.

2.3.1. Elementary effects method A modified EE method proposed by Campolongo et al. [14] is used to identify the significant parameters from a set of inputs. EE method employs a one-at-a-time (OAT) approach, wherein a single input parameter is varied while keeping all other parameters constant. The derivative of the change in the output quantity is calculated based on the change in the input parameter that gives the EE value. The EE value indicates the sensitivity level, i.e., the higher EE value for a given input parameter represents higher sensitivity.

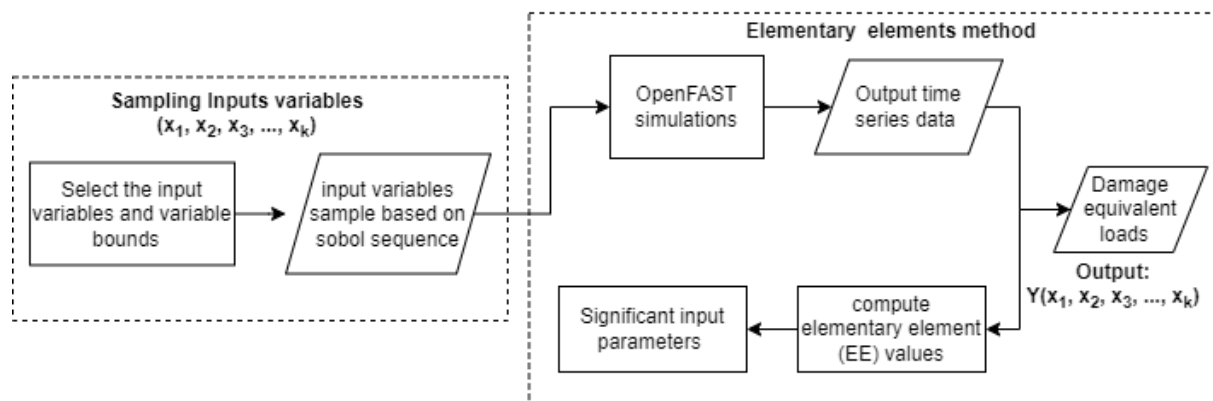


Figure 2: Schematic of the sensitivity analysis framework

While OAT approaches are typically considered local sensitivity methods, the EE method can overcome this limitation and become a global sensitivity method. This is accomplished by implementing the method at multiple points within the parameter hyperspace. The variation of parameters in the parameter hyperspace is achieved using either the radial method or the trajectory method, as shown in Figure 3a and 3b, respectively. In this work, the radial method is used. The global EE method [14] is also widely known as the Morris screening method and is detailed as follows:

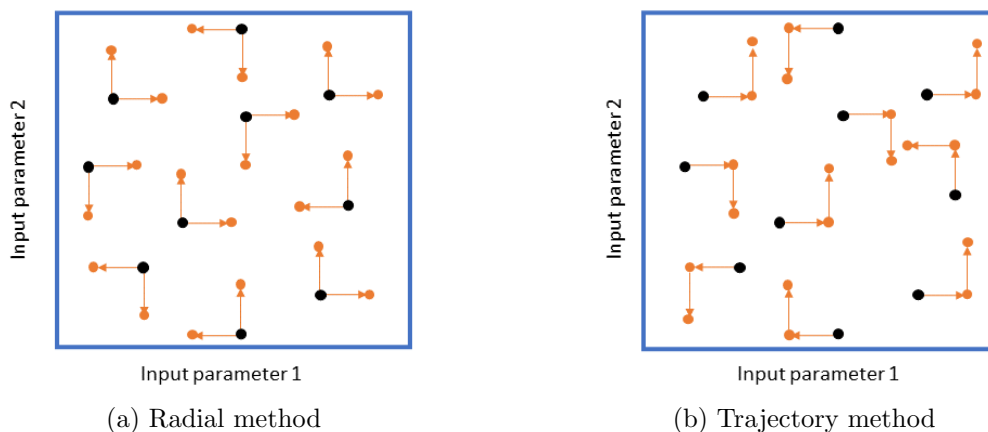


Figure 3: Sampling strategies. For a two-dimensional input parameter space, the black dots represent the starting points, and the orange points indicate the variation (of $\pm\Delta$) in one parameter at a time.

- The selected input parameter bounds are normalised such that k input parameters ($X_1, X_2, X_3, \dots, X_k$) lie between 0 and 1. R -starting points are sampled using quasi-random Sobol' sequences [15] for R starting points to achieve uniformly distributed input hyperspace.
- Outputs $Y(X_1, X_2, X_3, \dots, X_k)$ is obtained by running OpenFAST simulations for a particular set of inputs. $Y_j(X_1, X_2, X_3, \dots, X_k)$ denotes the j^{th} output in a multidimensional output space.

- The original Morris screening was proposed for a one-dimensional output space. However, it can be easily extended to account for multiple outputs. The EE value of input parameter X_i on Y_j is given by Equation 1, which indicates the sensitivity level of parameter X_i on output Y_j .

$$EE_{ij}^n = \frac{Y_j(X_1, X_2, \dots, X_i + \Delta_i, \dots, X_k) - Y_j(X_1, X_2, \dots, X_i, \dots, X_k)}{\Delta_i} \quad (1)$$

where Δ_i is the increment in input variable X_i . Each parameter is varied by about 10% of the value, i.e., $\Delta_i = 0.1$. These EE values are computed at R starting points, and n denotes each of these starting points.

- The mean EE and standard deviation denoted in Equation 2 are typically used as the sensitivity measures. However, this study uses a modified mean EE value given by Equation 3, as suggested by Campolongo et al. [14], to indicate sensitivity level.

$$\mu_{ij} = \frac{\sum_{n=1}^R EE_{ij}^n}{R}; \quad \sigma_i = \sqrt{\frac{\sum_{n=1}^R (EE_{ij}^n \mu_{ij})^2}{R-1}} \quad (2)$$

$$\mu_{ij}^* = \frac{\sum_{n=1}^R |EE_{ij}^n|}{R} \quad (3)$$

where μ_i is the mean EE and σ_i is the standard deviation of the EE. The standard deviation measures the extent of interactions and non-linear effects of each factor.

- The screening method is further refined to scale the elementary effects to compare the analysis reliably results on different outputs and prevent misleading rankings of the critical input parameters. Sin and Gernaey [16] introduced the Standardised elementary effects (SEE), which are scaled by the standard deviation of outputs, σ_{yj} , and input parameters, σ_{xi} , as follows:

$$SEE_{ij}^n = EE_{ij}^n \frac{\sigma_{xi}}{\sigma_{yj}} \quad (4)$$

2.3.2. Input variables and variable bounds The input variables under consideration in this study are summarised in Tables 1 and 2, including their respective lower and upper bounds.

The turbulence intensity (*TI*) bounds are expressed as a function of mean wind speed, as specified by Dimitrov et al. [17]. Class A turbulence is considered. The significant wave height and peak wave period are conditionally parameterised, as they depend on wind conditions and wind-wave misalignment. A lower bound function f_L and an upper bound function f_U define the wave parameter bounds. JONSWAP wave spectrum is determined using the significant wave height, peak period, and wave spectral shape factor. The uncertainty in spectral shape factor (γ) is not considered. It is instead regarded as functions of wave height and period given by Equation 5, as recommended by the IEC 61400-3-2 standard [2]. In this case, the wind direction aligns with the rotor direction. Therefore, the wave direction is equivalent to the wind-wave misalignment. The maximum current speed is determined based on the extreme site condition West of Barra, as outlined in the LIFES50+ report [18]. The system and structural properties are unaccounted for due to their low sensitivities observed by Wiley et al. [10]. Furthermore, water depth (320 m for spar-buoy and 200 m for semisubmersible) and water density (1025 kgm^{-3}). In other words, the uncertainty in water depth and water density is not accounted for as Wiley et al. [10] didn't notice any influence of these parameters.

$$\gamma = \begin{cases} 3.6, & \text{if } \frac{T_p}{\sqrt{H_s}} \leq 3.6, \\ 5.75 - 1.15 \frac{T_p}{\sqrt{H_s}}, & \text{if } 3.6 < \frac{T_p}{\sqrt{H_s}} < 5, \\ 1.0, & \text{if } \frac{T_p}{\sqrt{H_s}} \geq 5.0. \end{cases} \quad (5)$$

All input variables, excluding the hydrodynamic drag coefficients, are based on the FOWT operating conditions and are independent of the floater type. The column and heave plate drag coefficient values are adopted from Wiley et al. [10] for the semisubmersible configuration. For the spar configuration, the drag coefficient bounds are determined based on the drag characteristics of the cylinder with the same diameter as the OC3-Hywind spar.

Variable	Symbol	Units	Lower Bound	Upper Bound
Wind Speed	U_∞	ms^{-1}	4	25
Turbulence Intensity	TI	%	2.5	$\frac{18}{U_\infty} (6.8 + 0.75U_\infty + 3(\frac{10}{U_\infty})^2)$
Wave Direction	$WaveDir$	deg ($^\circ$)	-180	180
Significant wave height	H_s	m	$f_L(U_\infty, WaveDir)$	$f_U(U_\infty, WaveDir)$
Wave peak period	T_p	s	$f_L(H_s)$	$f_U(H_s)$
Current speed	U_{curr}	ms^{-1}	0	2
Current direction	$CurrDir$	deg ($^\circ$)	-180	180

Table 1: Wind-inflow, wave and current characteristics and the respective variable bounds

Variable	OC4-DeepCwind semisubmerible			OC3-Hywind spar		
	Symbol	Lower Bound	Upper Bound	Symbol	Lower Bound	Upper Bound
Drag Coefficient - Column	$C_{d_{top}}$	0.4	2	C_d	0.4	2.0
Drag Coefficient - Heave plate	$C_{d_{bottom}}$	0.4	3			
Axial drag coefficient	$C_{d_{ax}}$	3.5	5.5			

Table 2: Hydrodynamic drag coefficients and their bounds

2.3.3. Outputs of interest Table 3 lists all the outputs examined in the sensitivity analysis. This study calculates only the short-term damage equivalent loads (DEL). 10-minute DEL values for tower base moments, tower top moments, hydrodynamic forces and moments, and mooring line tension are computed from the output time history obtained from OpenFAST simulations. DELs are calculated using Palmgren Miner's rule, which depends on the number of cycles in a given time series and the Wöhler slope (slope of the S-N curve for specific material). The cycles in a given time series are computed using the Rainflow counting [19] algorithm. The Wöhler slope for different components of the FOWT system are: 3.5 for the tower, 10 for blade flapwise and 8 for blade edgewise moments, 3 for mooring lines, and 3 for substructure [20].

Outputs of interest	
Blade-root moments	Hydrodynamic forces
Yaw bearing bending moment	Hydrodynamic moments
Tower-base moment	Mooring line tension

Table 3: Output quantities of interest considered for the sensitivity analysis

3. Results

3.1. Significant parameter analysis - spar-buoy vs. semisubmersible

The sensitivity analysis is performed with eight input parameters for a 5MW baseline turbine with spar-buoy configuration and ten input parameters for semisubmersible configuration. This difference is due to the fact that only one drag coefficient represents the entire system for the spar, whereas three drag coefficients are used for the semisubmersible. Two wind inflow conditions generate a turbulent wind field in TurbSim, running 900 (30 starting points \times (1 + 2 wind inflow parameters) \times 10 seeds) TurbSim simulations each. 2700 OpenFAST (30 starting points \times (1 + 8 wind inflow parameters) \times 10 seeds) for spar-buoy and 3300 OpenFAST simulations (30 starting points \times (1 + 10 wind inflow parameters) \times 10 seeds) for semisubmersible are performed to obtain the significant parameter rankings.

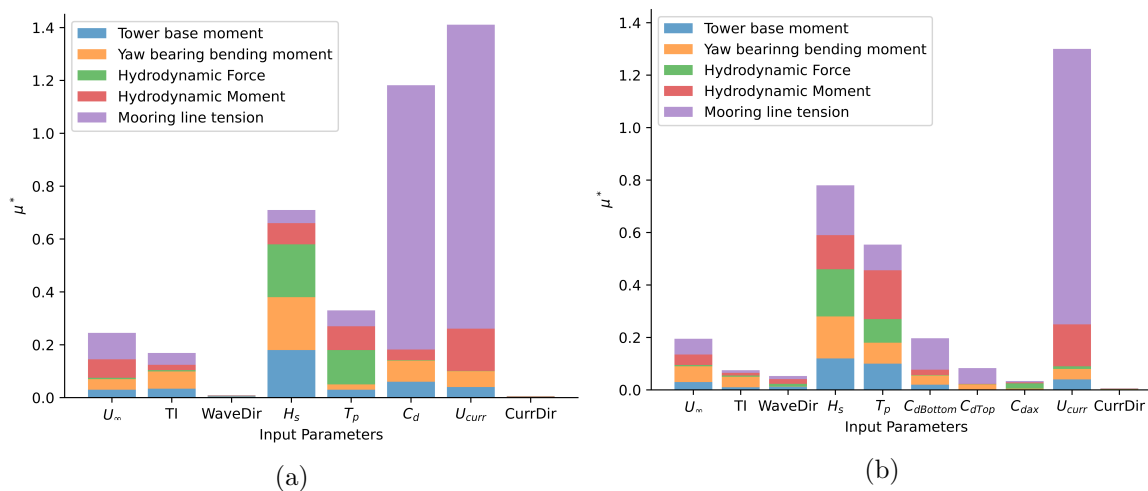


Figure 4: Significant input parameters for (a) OC3-Hywind Spar, (b) OC4-DeepCwind semisubmersible. Outputs represented in the plot are resultant forces and moments

The results identifying the significant input parameters for the spar and semisubmersible floating wind turbine are depicted in Figure 4a and 4b, respectively. Turbulence intensity and drag coefficients have a greater impact for spar type compared to the semisubmersible, while the rest of the input variables indicate similar sensitivities. The spar floater reduces wave loads and improves motion as it is slender in nature. This behaviour is reflected in the predominant impact of drag on mooring loads. In contrast, the motion of semisubmersible floaters, being inertia-dominant, renders the drag coefficient less influential on mooring loads compared to spar types. Moreover, the drag coefficients of the heave plates ($C_{dbottom}$) are more important than the drag coefficient of the columns (C_{dtop}) due to the additional viscous effects induced by heave plates. This trend aligns with observations made by Wiley et al. [10]. Wave characteristics

such as significant wave height (H_s) and wave period (T_p) exert less influence on the OC3-wind floater compared to the OC4-DeepCwind floater, where these parameters have a more substantial impact on hydrodynamic moments and mooring loads. Regardless of floater type, current velocity stands out as the most significant parameter. However, its major implication is on mooring loads, with comparatively minor effects on turbine and hydrodynamic loads. Notably, wind and wave misalignment (represented by wave direction) and current direction exhibit no discernible influence on mooring loads, possibly attributed to the symmetry of the mooring line arrangement. The mooring line tension is higher because it represents resultant tension rather than individual fairlead or anchor tension.

It is important to note that the current findings consider a single-point occurrence of wind and wave operating conditions and do not account for the probability of occurrence, which could result in different sensitivity rankings.

3.2. Influence of hydrodynamic model fidelity

Within HydroDyn, multiple approaches can be used to calculate the hydrodynamic loads on the floating platform - potential flow theory, strip-theory solution, or a hybrid combination of both. In this study, the focus is on hybrid theory with a first-order potential flow theory. However, more accurate hydrodynamics can be provided by accounting for the second-order loads in the form of difference and sum-frequency terms derived from the quadratic transfer functions (QTFs). The hydrodynamic coefficients required for the potential flow theory (both first and second-order) are computed using a frequency-domain solver (in this case, WAMIT). In this section, these two hydrodynamic models are compared to understand the consequences of the fidelity of the numerical model. The second-order WAMIT coefficients were computed at zero wave heading, and hence, wave direction is removed as an input parameter to avoid further computations. Figure 5 shows that the order of critical input parameters does not depend on the hydrodynamic model. However, there is a marginal impact on the mean EE value.

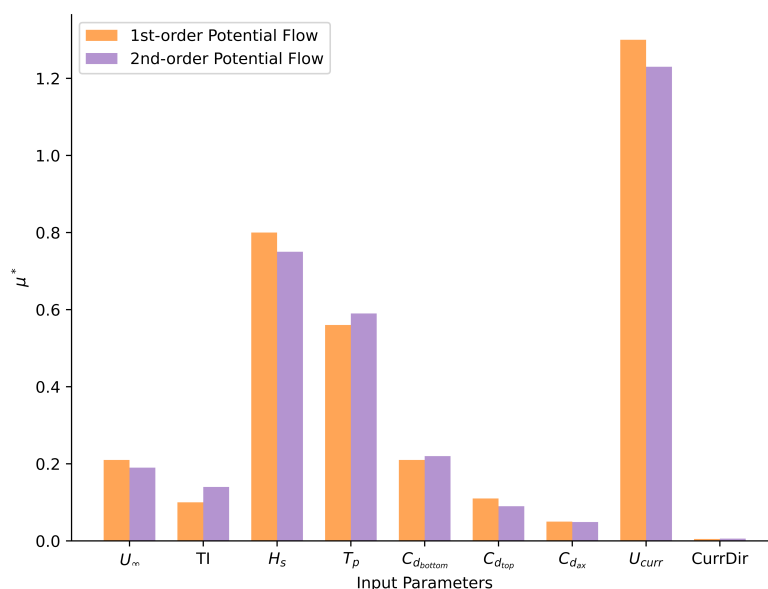


Figure 5: Significant input parameters with 1st-order and 2nd-order potential flow model for floater hydrodynamics

3.3. Trajectory convergence

The selection of the number of starting points (trajectories), R , sampled through the radial method is pivotal to ensure global sensitivity. In other words, by increasing the number of trajectories, no noticeable disparity is observed in the mean EE values associated with each input parameter and output. In this study, 30 trajectories are chosen. Therefore, a trajectory convergence is conducted for the semisubmersible floater to ensure that 30 trajectories are sufficient for accurate assessments. The number of trajectories varies from 0 to 30 points, eliminating the need for additional simulations. For each specified trajectory number ($R=1$ to 30), the corresponding mean EE values are computed at each input variable. These calculated values are then graphically represented for various DEL outputs in Figure 6. While the tower base and mooring loads stabilise after 10 trajectories, hydrodynamic and yaw-bearing loads require 15 trajectories to reach a steady value across all inputs. This indicates that using 30 starting points is sufficient for the present case. Additionally, the choice of starting points also depends on the nature of the output loads evaluated, as ultimate loads require more starting points to reach convergence, as shown by Wiley et al. [10].

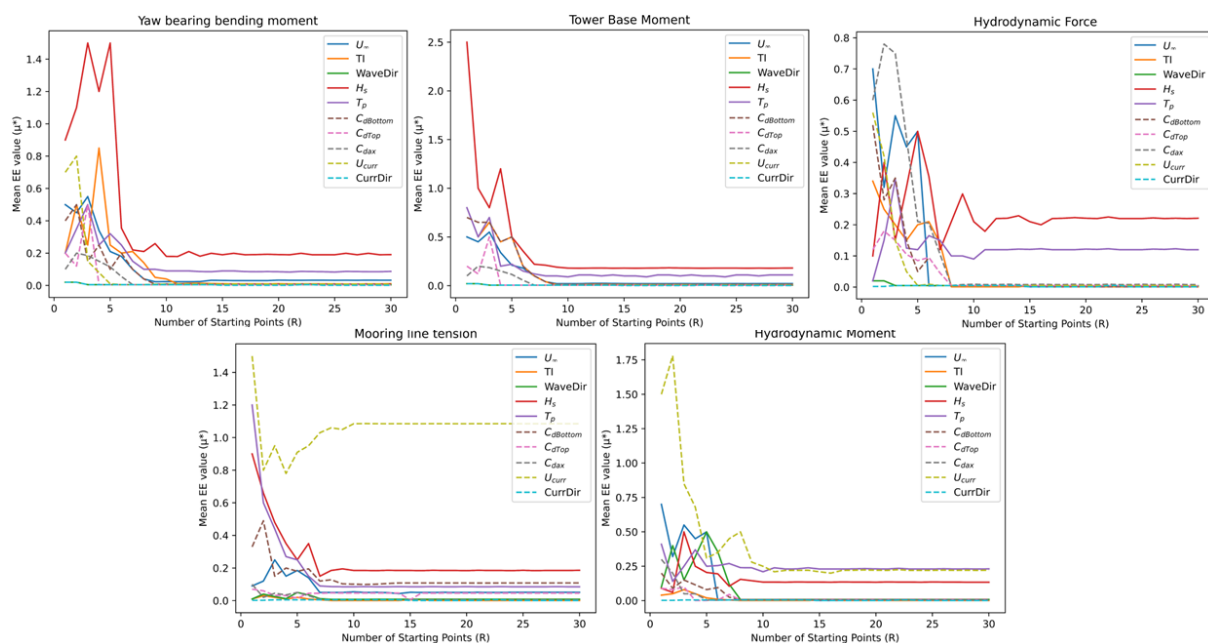


Figure 6: Trajectory convergence of mean EE value (μ^*) for each input parameters at different DEL outputs

4. Conclusions

An EE analysis of the wind inflow and turbine operating conditions was performed with the baseline NREL 5MW turbine atop two floating platform configurations. The order of sensitivity of different input variables was ranked for FOWTs with the semisubmersible and spar substructures. Some of the notable observations are summarised as follows:

- The order and level of sensitivities are specific to the floater type. If the rotor aerodynamics change, the results would be turbine-specific, too.
- The fidelity of the physical model for the hydrodynamics of the floating wind system has negligible impact on ranking the significant modelling parameters. Although the same

behaviour can be expected for rotor aerodynamics, conclusive statements cannot be made until a more thorough analysis is conducted.

- In employing the Morris screening method, choosing starting points crucially ensures a global sensitivity approach. This is obtained from a convergence study on starting points.
- The most significant parameters for NREL 5MW turbine atop an OC3-Hywind spar are current velocity, drag coefficient, significant wave height, and wave peak period.
- The key parameters for a 5MW baseline turbine affixed on an OC4-DeepCwind semisubmersible are current velocity, significant wave height, wave peak period, and drag coefficients of heave plates. Depending on the output loads considered, the sensitivity rankings will change.
- Maintaining consistent rotor aerodynamics for both floater types, notable distinctions between the two floater types are primarily with wave inflow conditions and drag coefficients.

As a future prospect, a similar study will be conducted on an IEA 15MW turbine, including a broader range of wind inflow parameters to capture the specifics of a larger, next-generation offshore wind turbine.

Acknowledgements

The project has received funding from the European Union's Horizon H2020 research and innovation programme under the Marie Skłodowska-Curie grant agreement No. 860737 (STEP4WIND project, step4wind.eu). The simulations used the Dutch national e-infrastructure with the support of the SURF Cooperative using grant No. EINF-1649.

Appendix A. Mooring system properties

Property	OC4-DeepCwind semisubmersible	OC3-Hywind spar
Number of mooring lines	3	3
Angle between adjacent lines	120°	120°
Depth to anchors below SWL	200 m	320 m
Depth to fairleads below SWL	14 m	70 m
Unstretched mooring line length	835.5 m	902.2 m
Mooring line diameter	0.0766 m	0.09 m
Equivalent mooring line mass density	113.35 kgm ⁻¹	77.7066 kgm ⁻¹
Equivalent mooring line mass in water	108.63 kgm ⁻¹	698.094 kgm ⁻¹
Equivalent mooring line extensional stiffness	753.6 MN	384.2 MN

Table A1: Mooring system properties

References

- [1] International Electrotechnical Commission, et al., IEC 61400-1: wind turbines part 1: design requirements, in International Electrotechnical Commission, 2005.
- [2] International Electrotechnical Commission, et al., IEC 61400-3: wind turbines part 3 - design requirements for offshore wind turbines, Wind Turbines-Part 3 (2009)
- [3] Tsvetkova O, Ouarda TB. A review of sensitivity analysis practices in wind resource assessment. Energy Conversion and Management. 2021 Jun 15;238:114112.
- [4] Velarde J, Kramhøft C, Sørensen JD. Global sensitivity analysis of offshore wind turbine foundation fatigue loads. Renewable energy. 2019 Sep 1;140:177-89.

- [5] Zhou S, Müller K, Li C, Xiao Y, Cheng PW. Global sensitivity study on the semisubmersible substructure of a floating wind turbine: Manufacturing cost, structural properties and hydrodynamics. *Ocean Engineering*. 2021 Feb 1;221:108585.
- [6] Fontana CM, Carswell W, Arwade SR, DeGroot DJ, Myers AT. Sensitivity of the dynamic response of monopile-supported offshore wind turbines to structural and foundation damping. *Wind Engineering*. 2015 Dec;39(6):609-27.
- [7] Rezaei R, Fromme P, Duffour P. Fatigue life sensitivity of monopile-supported offshore wind turbines to damping. *Renewable energy*. 2018 Aug 1;123:450-9.
- [8] Ziegler L, Voormeeren S, Schafhirt S, Muskulus M. Sensitivity of wave fatigue loads on offshore wind turbines under varying site conditions. *Energy Procedia*. 2015 Jan 1;80:193-200.
- [9] Robertson AN, Shaler K, Sethuraman L, Jonkman J. Sensitivity analysis of the effect of wind characteristics and turbine properties on wind turbine loads. *Wind Energy Science*. 2019 Sep 10;4(3):479-513.
- [10] Wiley W, Jonkman J, Robertson A, Shaler K. Sensitivity Analysis of Numerical Modeling Input Parameters on Floating Offshore Wind Turbine Loads. *Wind Energy Science Discussions*. 2023 May 15;2023:1-35.
- [11] Jonkman J, Butterfield S, Musial W, Scott G. Definition of a 5-MW reference wind turbine for offshore system development (No. NREL/TP-500-38060). National Renewable Energy Lab.(NREL), Golden, CO (United States); 2009 Feb 1.
- [12] Jonkman J. Definition of the Floating System for Phase IV of OC3 (No. NREL/TP-500-47535). National Renewable Energy Lab.(NREL), Golden, CO (United States); 2010 May 1.
- [13] Robertson A, Jonkman J, Masciola M, Song H, Goupee A, Coulling A, Luan C. Definition of the semisubmersible floating system for phase II of OC4. National Renewable Energy Lab.(NREL), Golden, CO (United States); 2014 Sep 1.
- [14] Campolongo F, Saltelli A, Cariboni J. From screening to quantitative sensitivity analysis. A unified approach. *Computer physics communications*. 2011 Apr 1;182(4):978-88.
- [15] Sobol' IY. On the distribution of points in a cube and the approximate evaluation of integrals. *Zhurnal Vychislitel'noi Matematiki i Matematicheskoi Fiziki*. 1967;7(4):784-802.
- [16] Sin G, Gernaey KV. Improving the Morris method for sensitivity analysis by scaling the elementary effects. In *Computer aided chemical engineering 2009* Jan 1 (Vol. 26, pp. 925-930). Elsevier.
- [17] Dimitrov N, Kelly MC, Vignaroli A, Berg J. From wind to loads: wind turbine site-specific load estimation with surrogate models trained on high-fidelity load databases. *Wind Energy Science*. 2018 Oct 24;3(2):767-90.
- [18] Yu W, Muller K, Lemmer F. Qualification of Innovative Floating Substructures for 10MW Wind Turbines and Water Depths Greater than 50m. University of Stuttgart, 2015
- [19] Amzallag C, Gery JP, Robert JL, Bahuaud J. Standardization of the rainflow counting method for fatigue analysis. *International journal of fatigue*. 1994 Jun 1;16(4):287-93.
- [20] Veritas DN. DNV-RP-C205 Environmental conditions and environmental loads. Det Norske Veritas: Oslo, Norway. 2010.